

Spin states and persistent currents in a mesoscopic ring with an embedded magnetic impurity

J. S. Sheng and Kai Chang*

SKLSM, Institute of Semiconductors, Chinese Academy of Sciences, P. O. Box 912, Beijing 100083, China

Spin states and persistent currents are investigated theoretically in a mesoscopic ring with an embedded magnetic ion under a uniform magnetic field including the spin-orbit interactions. The magnetic impurity acts as a spin-dependent δ -potential for electrons and results in gaps in the energy spectrum, consequently suppresses the oscillation of the persistent currents. The competition between the Zeeman splittings and the s - d exchange interaction leads to a transition of the electron ground state in the ring. The interplay between the periodic potential induced by the Rashba and Dresselhaus spin-orbit interactions and the δ -potential induced by the magnetic impurity leads to significant variation in the energy spectrum, charge density distribution, and persistent currents of electrons in the ring.

PACS numbers: 73.23.Ra, 71.70.Ej, 71.70.Gm, 75.50.Pp

I. INTRODUCTION

Recently, spin dependent optical and transport properties of semiconductors have received renewed interest due to the potential applications of spintronic devices.^{1,2} One of the essential requirements in a spintronic device is to generate spin-polarized current. In a diluted magnetic semiconductor (DMS), the s - d exchange interaction³ between the electrons and the magnetic impurities makes it possible to tailor electron spin splitting and thereby generate spin-polarized currents^{4,5,6,7}.

The spin states of the electrons in a semiconductor can also be manipulated by an external electric field via the spin-orbit interaction (SOI). There are two types of SOI's in semiconductors. One is the Rashba spin-orbit interaction (RSOI) induced by structure inversion asymmetry,^{8,9} and the other is the Dresselhaus spin-orbit interaction (DSOI) induced by bulk inversion asymmetry¹⁰. The strength of the RSOI can be tuned by external gate voltages or asymmetric doping, while the strength of the DSOI is inversely proportional to the thickness of the quantum well and thus becomes comparable with that of RSOI in narrow quantum wells.¹¹ SOI makes it possible to generate a spin current (SC) electrically without the use of ferromagnetic material or a magnetic field.^{12,13} The impact of in-plane magnetic field on the spin hall conductivity has been investigated in the two-dimensional electron gas (2DEG) in the presence of both the RSOI and DSOI.¹⁴ The coexisting of the s - d exchange interaction and spin-orbit interactions in 2DEG could result in a significant change of the spin polarization of the charge current (CC).¹⁵

Recent progress in fabrication techniques makes it possible to dope a few or even one magnetic impurity in a semiconductor nanostructure.¹⁶ Aharonov-Bhomb oscillations and spin-polarized transport properties in a mesoscopic open ring with an embedded magnetic impurity have been investigated theoretically¹⁷ using quantum wave-guide theory¹⁸ without spin-orbit interactions. Persistent charge and spin currents in closed mesoscopic rings in the presence of a nonmagnetic impurity were studied including the RSOI,¹⁹ and a rounding effect of the nonmagnetic impurity on the energy spectrum and the flux oscillation of the persistent CC was found. However, it is interesting to investigate the effect of a magnetic impurity

on persistent currents, especially spin current, in a mesoscopic ring. The interplay between the RSOI and DSOI can induce an effective azimuthal periodic potential in the ring, consequently breaks the cylindrical symmetry of the ring,²⁰ and this feature makes the spin states and the persistent currents depend sensitively on the position of the magnetic impurity.

In this work, we study spin states and persistent currents of a 1D mesoscopic ring with an embedded magnetic impurity in the presence of both the RSOI and DSOI. The interplay between the Zeeman splittings and the s - d exchange interaction leads to a transition of the electron ground state. The energy spectrum and the persistent currents depend sensitively on the position of the magnetic impurity including both the RSOI and DSOI, since the interplay between the RSOI and DSOI breaks the cylindrical symmetry. It is interesting to notice that the symmetry of the persistent SC in the parameter space (α - β) is robust against the magnetic impurity. The paper is organized as follows. The theoretical model is presented in Sec. II. The numerical results and discussion are given in Sec. III. Finally, we give a brief conclusion in Sec. IV.

II. THEORETICAL MODEL

In the presence of both the RSOI and DSOI, the dimensionless Hamiltonian of a mesoscopic ring with an embedded magnetic impurity (see Fig. 1) under a uniform perpendicular magnetic field reads²⁰

$$H = \left[-i \frac{\partial}{\partial \varphi} + \phi + \frac{\alpha}{2} \sigma_r - \frac{\beta}{2} \sigma_\varphi(-\varphi) \right]^2 - \frac{\alpha^2 + \beta^2}{4} + \frac{\alpha\beta}{2} \sin 2\varphi + g_e \phi \sigma_z^e + g_m \phi \sigma_z^m - 2\pi J \hat{s}^e \cdot \hat{s}^m \delta(\varphi - \theta), \quad (1)$$

where ϕ is the magnetic flux in the units of $\phi_0 = h/e$, and α and β specify the strengths of the RSOI and DSOI, respectively. $\sigma_r = \cos \varphi \sigma_x^e + \sin \varphi \sigma_y^e$ and $\sigma_\varphi = \cos \varphi \sigma_y^e - \sin \varphi \sigma_x^e$, g_e (g_m) is the g factor of the electron (magnetic impurity), and J is the strength of the s - d exchange interaction between the conduction band electron \hat{s}^e and the magnetic impurity \hat{s}^m . As discussed in our previous work, the interplay between the RSOI and DSOI induces a $\sin 2\varphi$ potential [the third term

III. NUMERICAL RESULTS AND DISCUSSION

A. The effects of the magnetic impurity

In order to clearly investigate the effects of the magnetic impurity on the spin states and persistent currents in the 1D ring, we first neglect the Zeeman splittings and spin-orbit interactions. The Hamiltonian of the system becomes

$$H = \left(-i \frac{\partial}{\partial \varphi} + \phi \right)^2 - 2\pi J \hat{s}^e \cdot \hat{s}^m \delta(\varphi - \theta). \quad (7)$$

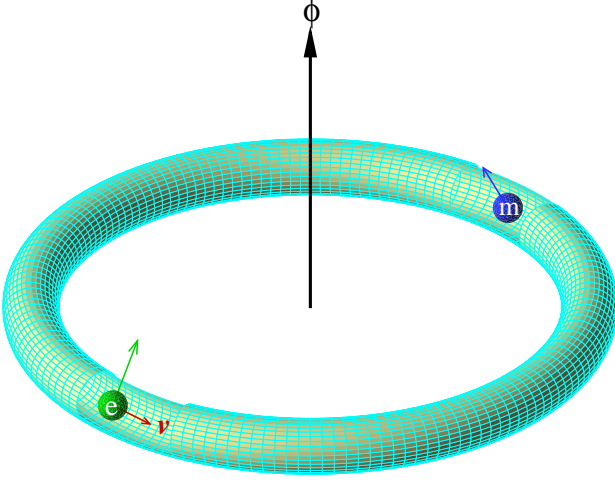


FIG. 1: (Color online) Schematic diagram for a mesoscopic ring with an embedded magnetic impurity.

The charge density operator and the charge current density operator are

$$\begin{aligned} \hat{\rho}(\varphi') &= -e\delta(\varphi' - \varphi) \\ \hat{j}_c(\varphi') &= \frac{1}{2}[\hat{\rho}(\varphi')\hat{v} + \hat{v}\hat{\rho}(\varphi')], \end{aligned} \quad (2)$$

where φ' refers to the field coordinates and φ the coordinates of the electron. The velocity operator associated with the Hamiltonian in Eq. (1) is

$$\hat{v} = \mathbf{e}_\varphi \left[-i \frac{\partial}{\partial \varphi} + \phi + \frac{\alpha}{2} \sigma_r - \frac{\beta}{2} \sigma_\varphi(-\varphi) \right]. \quad (3)$$

We can also introduce the spin density and spin current density operators as

$$\begin{aligned} \hat{S}(\varphi') &= \hat{s}^e \delta(\varphi' - \varphi) \\ \hat{j}_s(\varphi') &= \frac{1}{2}[\hat{S}(\varphi')\hat{v} + \hat{v}\hat{S}(\varphi')], \end{aligned} \quad (4)$$

where \hat{s}^e is the vector of the electron spin operator. The charge current density and spin current density can be obtained by calculating the expectation values of the corresponding operators:

$$\begin{aligned} j_c(\varphi') &= \langle \Psi | \hat{j}_c | \Psi \rangle = -e \text{Re} \{ \Psi^\dagger(\varphi') \hat{v}' \Psi(\varphi') \} \\ j_s(\varphi') &= \langle \Psi | \hat{j}_s | \Psi \rangle = \text{Re} \{ \Psi^\dagger(\varphi') \hat{v}' \hat{s}^e \Psi(\varphi') \}, \end{aligned} \quad (5)$$

where $\Psi(\varphi)$ is the wavefunction of an electron in the ring. For convenience, we note φ' and \hat{v}' as φ and \hat{v} hereafter.

The azimuthal (spin or charge) current can be defined as²¹

$$I = \frac{1}{2\pi} \int_0^{2\pi} d\varphi j(\varphi). \quad (6)$$

At low temperature, N electrons will occupy the lowest N levels of the energy spectrum. The total (charge or spin) current is the summation over all occupied levels.¹⁹

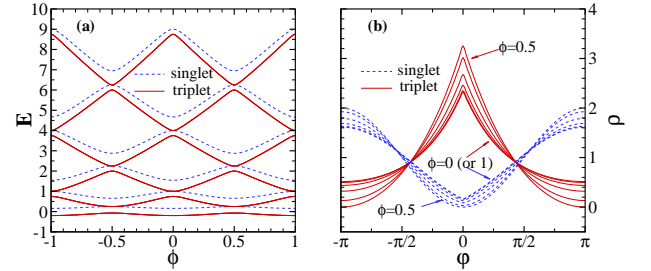


FIG. 2: (Color online) (a) Energy spectrum of 1D mesoscopic ring with one magnetic impurity at different magnetic fluxes; (b) Probability density distribution for the lowest triplet and singlet states of 1D ring with one magnetic impurity for different magnetic flux. $J = 0.5$ and $\theta = 0$.

When a spin-1/2 magnetic impurity appears in the mesoscopic ring, the total angular momentum of the eigenstates is equal to 1 (triplet) or 0 (singlet) due to the coupling between the electron spin \hat{s}^e and the impurity spin \hat{s}^m . In the coupling representation, the Hamiltonian can be written as

$$H_c = \begin{bmatrix} H_S & 0 \\ 0 & H_T I_3 \end{bmatrix}, \quad (8)$$

where $H_S = \left(-i \frac{\partial}{\partial \varphi} + \phi \right)^2 + \frac{3\pi J}{2} \delta(\varphi - \theta)$ is the Hamiltonian for the singlet states ($j = 0$), $H_T = \left(-i \frac{\partial}{\partial \varphi} + \phi \right)^2 - \frac{\pi J}{2} \delta(\varphi - \theta)$ is the Hamiltonian for the triplet states ($j = 1$), and I_3 represents the 3×3 identity matrix. We can find that the magnetic impurity behaves like a barrier (well) for the singlet (triplet) state when $J > 0$.

Fig. 2(a) shows the energy spectrum of the mesoscopic ring with an embedded magnetic impurity. The energy splittings between the triplet and singlet states are proportional to the strength of the exchange interaction $J > 0$. The neighboring singlet and triplet levels can degenerate at special magnetic fluxes (integer or half-integer ϕ). When ϕ is an integer, the energies of the fourfold degenerate levels are $1, 4, 9, \dots, n^2, \dots$, which can be obtained from $\sin \pi \kappa = 0$ in both Eq. (A.6) and Eq. (A.10) in the Appendix; When ϕ is a half-integer, the energies of the fourfold degenerate levels are $1/4, 9/4, 25/4, \dots, (n + 1/2)^2, \dots$, which can be obtained

from $\cos \pi \kappa = 0$ in both Eq. (A.7) and Eq. (A.11) in the Appendix.

Note that the orbital wavefunction and spin wavefunction can be separated in the ring without SOI. The eigenstates of the system can be written as $\Psi = X_{jm}(\varphi)|\frac{1}{2}\frac{1}{2}jm\rangle$ where $j = 0, 1$ and $m = -j, \dots, j$. The orbital wavefunctions X_{jm} are determined by

$$\left(-i\frac{\partial}{\partial\varphi} + \phi\right)^2 X_{00} + \frac{3}{2}\pi J\delta(\varphi - \theta)X_{00} = EX_{00}, \quad (9a)$$

$$\left(-i\frac{\partial}{\partial\varphi} + \phi\right)^2 X_{1m} - \frac{1}{2}\pi J\delta(\varphi - \theta)X_{1m} = EX_{1m}. \quad (9b)$$

This means that the spin-1/2 magnetic impurity acts as a δ -barrier (well) and well (barrier) on the singlet and triplet states for $J > 0$ ($J < 0$), respectively. This feature consequently leads to different localization of the singlet and triplet states [see Fig. 2(b)]. We assume $J > 0$ in this work without loss of generality. In this case, the ground state of the system is a triplet state.

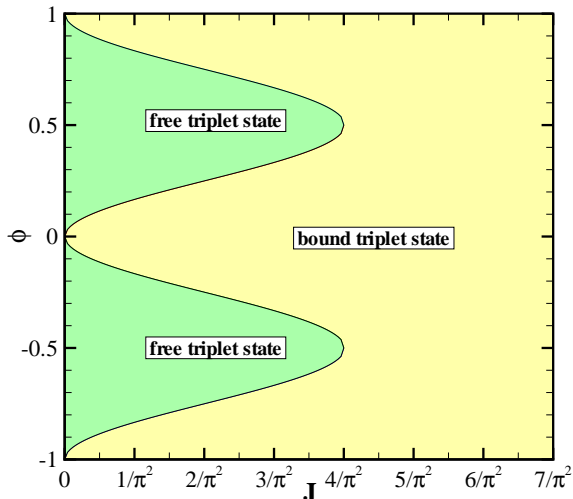


FIG. 3: (Color online) The phase diagram of the ground triplet state in the ring at different magnetic flux ϕ and s - d exchange interaction strength J .

We now focus on the lowest triplet state. The transition between bound state and free state can be clearly seen in Fig. 3 as a function of the magnetic flux ϕ and the strength of the s - d exchange interaction J . The lowest triplet state is a bound state at an integer ϕ because Eq. (A.13) has one solution for any given positive J . Whether the lowest triplet state at a half-integer ϕ is a bound state ($E < 0$) or free state ($E > 0$) depends on the strength of the s - d exchange interaction J . When $J > 4/\pi^2$, Eq. (A.14) has a nontrivial solution, and therefore the lowest triplet state at a half-integer ϕ is a bound state. When $J < 4/\pi^2$, Eq. (A.14) only has a trivial solution, and thus the lowest triplet state at a half-integer ϕ is a free state. This means that when the strength of the s - d exchange interaction J is not large enough ($0 < J < 4/\pi^2$), the triplet ground

state changes from bound state to free state while varying the magnetic flux ϕ . However, when J is large enough, ($J > 4/\pi^2$) the ground state electron is always trapped by the magnetic impurity at any magnetic flux ϕ .

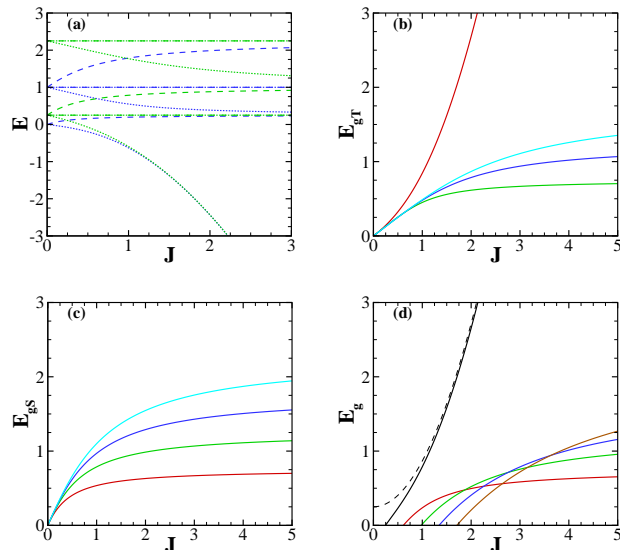


FIG. 4: (Color online) (a) The lowest triplet (dotted) and singlet (dashed) energy levels as functions of the s - d exchange interaction strength J . The blue (green) lines are for the integer (half-integer) magnetic flux ϕ ; (b) The lowest four triplet gaps as functions of J , where the red (green, blue, cyan) line denotes the first (second, third, fourth) lowest singlet gap; (c) The same as (b) but for the singlet gaps; (d) The true energy gaps as functions of the s - d exchange interaction strength J . The dark (red, green, blue, brown) line denotes the first (second, third, fourth, fifth) lowest energy gap. The dashed line depicts the asymptotic behavior of the lowest energy gap as J increases.

Fig. 4(a) depicts the lowest triplet (dotted) and singlet (dashed) energy levels as functions of the strength of the s - d exchange interaction J at an integer magnetic flux (blue) or half-integer magnetic flux (green). The dash-dotted horizontal lines correspond to those special fourfold degenerate points in Fig. 2(a) whose energies do not change with J . The energy difference of two triplet (or singlet) states at different magnetic fluxes but of the same order approach zero as $J \rightarrow \infty$, e.g.,

$$\begin{aligned} E_{T1}(\phi = 0) &\rightarrow E_{T1}(\phi = 1/2) \rightarrow -\pi^2 J^2 / 16 \\ E_{S1}(\phi = 0) &\rightarrow E_{S1}(\phi = 1/2) = 1/4 \\ E_{T2}(\phi = 0) &\rightarrow E_{T2}(\phi = 1/2) = 1/4 \\ E_{S2}(\phi = 1/2) &\rightarrow E_{S2}(\phi = 0) = 1 \\ E_{T3}(\phi = 1/2) &\rightarrow E_{T3}(\phi = 0) = 1 \end{aligned}$$

as $J \rightarrow \infty$. These results can be obtained from approximate solutions to the three transcendental equations, i.e., Eqs. (A.5), (A.9) and (A.12) in the Appendix, for large J at integer and half-integer magnetic flux. The lowest four energy gaps between triplet (singlet) states are shown in Fig. 4(b) [Fig. 4(c)]. But they are only pseudo gaps. The true gaps are shown in

Fig. 4(d), the energy gaps appear successively and increase. The lowest energy gap $E_{g1} = E_{S1}(\phi = 0) - E_{T1}(\phi = 1/2)$ approaches $1/4 + \pi^2 J^2/16$ as $J \rightarrow \infty$ [see the dashed line in Fig. 4(d)], and the second lowest energy gap $E_{g2} = E_{S2}(\phi = 1/2) - E_{T2}(\phi = 0)$ approaches $1 - 1/4 = 3/4$ as $J \rightarrow \infty$. The third, fourth, and fifth lowest energy gaps approach $5/4$, $7/4$, and $9/4$ as $J \rightarrow \infty$, respectively.

Fig. 5(a) shows the persistent CC's from the lowest triplet and singlet energy levels at different magnetic flux ϕ . The persistent CC from both the triplet and singlet states are smoothed and suppressed by the magnetic impurity. The persistent SC's from the lowest $|1, -1\rangle$, $|1, 0\rangle$, $|1, 1\rangle$, and $|0, 0\rangle$ are depicted in Fig. 5(b). The SC contributions of $|1, 0\rangle$ and $|0, 0\rangle$ are always zero and the SC contributions of $|1, -1\rangle$ and $|1, 1\rangle$ are always opposite, thus canceling each other. We note that the persistent SC from the lowest $|1, -1\rangle$ is proportional to the persistent CC from the same state. The oscillation amplitudes, i.e., the maximal values, of the persistent CC from the lowest triplet and singlet energy levels are shown in Fig. 5(c) with different strengths of the s - d exchange interaction J . The persistent CC's from both the lowest triplet and singlet energy levels decline as J increases. We recall that the magnetic impurity acts as a δ -well (δ -barrier) for the triplet (singlet) states. Both the δ -well and δ -barrier hinder electron propagation along the ring and suppress the persistent CC (and SC). The persistent CC from the lowest triplet energy level declines more rapidly than its singlet counterpart because the electron is more localized (around the δ -well) for the triplet states than for the singlet states. Nevertheless, for small J the persistent CC from the lowest singlet energy level can be smaller than that from the lowest triplet energy level [see Fig. 5(a)] because the strength of the δ -barrier for the singlet states is triple the strength of the δ -well for the triplet states.

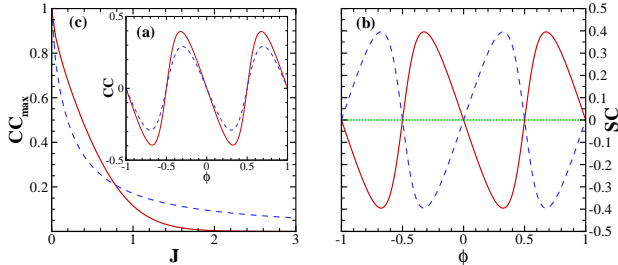


FIG. 5: (Color online) (a) The persistent CC from the lowest triplet (singlet) energy level at different magnetic flux ϕ is denoted by the red solid (blue dashed) line, $J = 0.5$; (b) The persistent SC from the lowest $|1, -1\rangle$ ($|1, 1\rangle$) state is denoted by the red solid (blue dashed) line, and the green dotted lines are the persistent SC from the lowest $|1, 0\rangle$ state and that from the lowest $|0, 0\rangle$ state, $J = 0.5$; (c) The maximal value of the persistent CC from the lowest triplet (singlet) energy level with different strengths of the s - d exchange J is denoted by red solid (blue dashed) line.

Now we include the intrinsic Zeeman terms of both the electron and the magnetic impurity, e.g., GaAs ring. The energy spectrum with an embedded spin-1/2 magnetic impurity is depicted in Fig. 6(a). The dimensionless g factors

$g_e = g_e^* m^* = -0.02948$ and $g_m = g_m^* m^* = 0.134$. It is interesting to notice that the $|0, 0\rangle$ states and $|1, 0\rangle$ states are coupled together by the Zeeman terms [see Eq. (A.16)]. Although these states are mixed, the projection of the angular momentum along the z -axis (\hat{j}_z) is still a good quantum number, i.e., $\langle \hat{j}_z \rangle = 0$ [see the red dotted lines in Fig. 6(a)]. The states $|1, -1\rangle$ and $|1, 1\rangle$ are decoupled, and the Zeeman terms only alter their energies [see the green dashed lines and the blue solid lines in Fig. 6(a)], while the total spin \hat{j} and its z -component \hat{j}_z are still good quantum numbers. Fig. 6(b) shows the phase diagram for the ground state of the ring at different J and ϕ . From this figure one can see that the ground state in the ring can transit among those three kinds of states due to the interplay between the Zeeman terms and s - d exchange interaction as the magnetic flux ϕ increases, and $\langle \hat{j}_z \rangle$ and $\langle \hat{s}_z \rangle$ undergo sudden changes across boundaries in the phase diagram [see the red and blue lines in Fig. 6(b)].

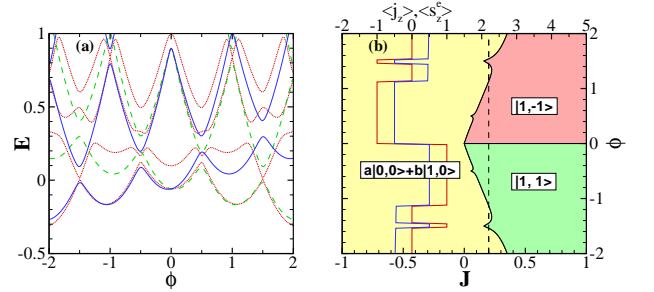


FIG. 6: (Color online) (a) Energy spectrum of a GaAs ring with an embedded spin-1/2 magnetic impurity ($J = 0.2$), the Zeeman terms of both the electron and the magnetic impurity are included, $g_e = -0.02948$ and $g_m = 0.134$, the red dotted lines denote those levels with zero $\langle \hat{j}_z \rangle$, and the green dashed (blue solid) lines denote the $|1, -1\rangle$ ($|1, 1\rangle$) levels; (b) The three-phase transition of the ground state, and the variations of the $\langle \hat{j}_z \rangle$ (the red line) and $\langle \hat{s}_z \rangle$ (the blue line) along the dashed line ($J = 0.2$), $\bar{g}_1 = -0.02948$ and $\bar{g}_2 = 0.134$.

B. The effects of the RSOI and DSOI

In this subsection, we focus on the competition between the s - d exchange interaction and SOIs. From Eq. (1), the interplay between the RSOI and DSOI induces a $\sin 2\phi$ periodic potential and breaks the cylindrical symmetry of the mesoscopic ring. The spin states, energy spectrum and persistent currents depend sensitively on the position of the magnetic impurity.

Fig. 7 depicts the influence of the position of the magnetic impurity on the eigenenergy spectrum of the mesoscopic ring in the presence of both the RSOI and DSOI. Strictly speaking, the degeneracy of the triplet states is lifted by the RSOI and DSOI. The position of the magnetic impurity more significantly influences the lower energy levels than the higher levels since the wavefunctions of the lower states are more localized than that of the higher states. In such an anisotropic ring, $\theta = 0$ and $\theta = \pm\pi/2$ are equivalent positions which can be connected to each other by mirror reflections with respect to the $\phi = \pm\pi/4$ planes, and therefore two energy spectra in

panels (a) and (d) in Fig. 7 are exactly the same. The energy splittings due to the s - d exchange interaction in panel (b) [(c)] are largest (smallest) because the probability density of the lowest bound states exhibits maxima (minima) when the magnetic impurity is located at the bottom (peak) of the $\sin 2\varphi$ periodic potential induced by the interplay between the RSOI and DSOI. We also notice that the corresponding energy splittings of the second bound state in panel (b) are zero because the magnetic impurity is located just at the node ($\theta = -\pi/4$) of the wavefunction of the second bound state.

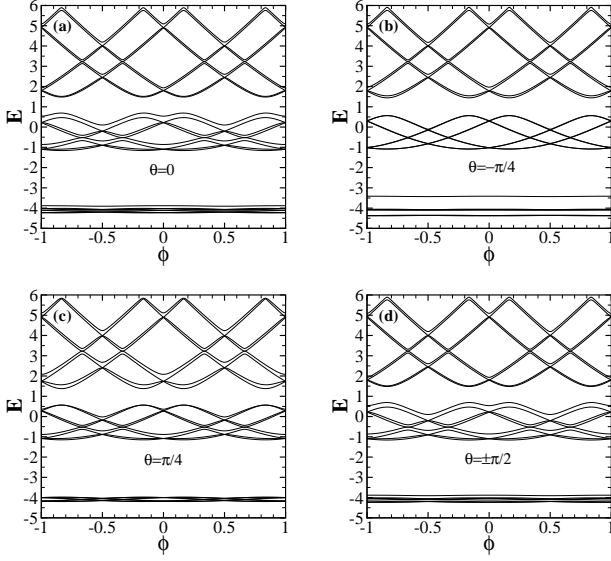


FIG. 7: Energy spectrum of 1D mesoscopic ring with an embedded spin-1/2 magnetic impurity and two types of SOI's, $J = 0.2$, $\alpha = 3$ and $\beta = 2$, the position of the impurity is $\theta = 0$ in panel (a), and $-\pi/4, \pi/4, \pm\pi/2$ in panel (b), (c), (d) respectively.

Fig. 8 shows the probability density distributions of the lowest singlet and triplet states for different positions of the magnetic impurity. The electron is distributed along the ring according to the potential $\frac{\alpha\beta}{2}\sin 2\varphi$, which is induced by the interplay between the RSOI and DSOI [see Eq. (1)] in the absence of a magnetic impurity. This potential $\frac{\alpha\beta}{2}\sin 2\varphi$ exhibits two valleys at $\varphi = -\pi/4$ and $\varphi = 3\pi/4$, where the electron is most likely to appear, and two peaks at $\varphi = \pi/4$ and $\varphi = -3\pi/4$, corresponding to the minimum of the probability density of electron. As shown in the previous subsection, the magnetic impurity acts as a δ -like barrier for the singlet state electron and as a δ -well for the triplet state electron when $J > 0$, and the height of the δ -barrier is three times larger than that of the δ -well [see Eq. (9)]. Thus the presence of the magnetic impurity will make the potential profile at the positions $\varphi = -\pi/4$ and $\varphi = 3\pi/4$ no longer equivalent. From Fig. 8 one can find that the competition between the magnetic impurity and SOIs, i.e., the probability density of an electron at the valley, is enhanced (reduced) for the triplet (singlet) state electron when the position of the magnetic impurity approaches the valley [see the black line in Fig. 8(a)]. It is interesting to note that the magnetic impurity acting as a δ -like barrier for

the singlet state could also enhance the probability density of the electron at the other valley ($\varphi = 3\pi/4$) when it is at the valley ($\varphi = 3\pi/4$) of the potential $\frac{\alpha\beta}{2}\sin 2\varphi$ [see the black line in Fig. 8(b)].

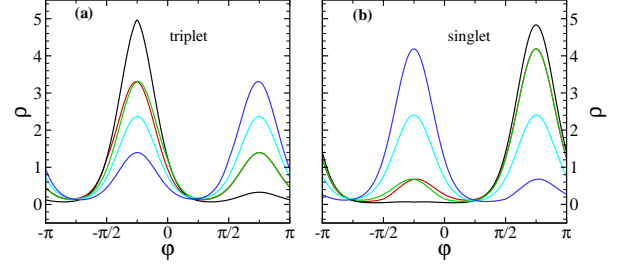


FIG. 8: (Color online) The probability density distributions of the lowest triplet [panel (a)] and singlet [panel (b)] states. The red (dark, green, cyan, blue) line is for the magnetic impurity located at $\theta = -\pi/2$ ($-\pi/4, 0, \pi/4, \pi/2$). Other parameters are $J = 0.2$, $\alpha = 3$, $\beta = 2$, and $\phi = 0$.

Two types of energy gaps appear in the energy spectrum of a mesoscopic ring, including the RSOI, the DSOI, and the s - d exchange interaction [see Fig. 9]. In our previous work²⁰, we discussed the energy gaps caused by the coexistence of the RSOI and DSOI (E_{g-I}). As shown in Fig. 4(d), the s - d exchange interaction can also open an energy gap (E_{g-II}) if the strength J is greater than the corresponding threshold value. We demonstrate in Fig. 10 that the two types of energy gaps tend to compete against each other. The lowest SOI induced gap declines as the strength of the s - d exchange interaction increases [see Fig. 10(a)]. That is because the energy splittings between singlet and triplet states caused by the s - d exchange interaction tend to squeeze the gap induced by SOI especially when the magnetic impurity approaches the valley of potential ($\theta = -\pi/4$) since the s - d exchange interaction is a contact interaction that depends on the overlap between the magnetic impurity and the electron. Fig. 10(b) depicts the energy gap induced by the s - d exchange interaction as a function of the strength of SOIs. The increasing strengths of the RSOI and DSOI enhance the localization of the electron. The gap increases when the magnetic impurity is located at the valley of the potential $\frac{\alpha\beta}{2}\sin 2\varphi$ ($\theta = -\pi/4$) as the SOI strengths (α and β) increase, or decrease when the magnetic impurity is at other sites. The gap width decreases most rapidly when the magnetic impurity locates at the peak of the potential $\frac{\alpha\beta}{2}\sin 2\varphi$ ($\theta = \pi/4$).

The s - d exchange interaction can also influence the persistent SC. In Fig. 11(a), we show a contour plot of the persistent SC as a function of the s - d exchange interaction strength J and the position of the magnetic impurity θ . We can see that the persistent SC oscillates with the magnetic impurity position θ when the strength J is fixed. The magnitude of the persistent SC exhibits maxima at $\theta = \pi/4, 3\pi/4, 5\pi/4, 7\pi/4$, where the valleys and peaks of the potential $\frac{\alpha\beta}{2}\sin 2\varphi$ are. There are also four specific positions of magnetic impurity [the white regions in Fig. 11(a)] where the magnitude of the persistent

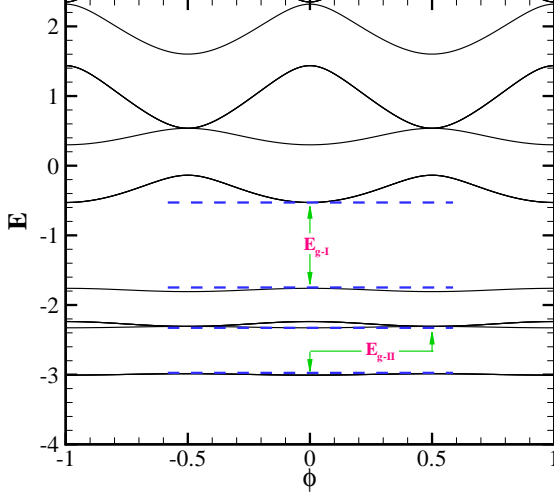


FIG. 9: (Color online) Two types of energy gaps appear in the energy spectrum while the spin-orbit interactions and $s-d$ exchange interaction coexist in the mesoscopic ring. E_{g-I} denotes the lowest (direct) energy gap induced by the RSOI and DSOI, E_{g-II} denotes the lowest (indirect) energy gap induced the $s-d$ exchange interaction. $\alpha = \beta = 2$, $J = 1$, $\theta = 0$.

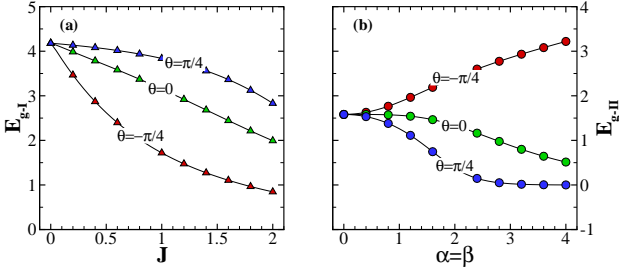


FIG. 10: (Color online) (a) The lowest SOI induced gap vs the $s-d$ exchange interaction strength J with different positions of the magnetic impurity, $\alpha = \beta = 3$; (b) The lowest $s-d$ induced gap vs the SOI strengths ($\alpha = \beta$) with different positions of the magnetic impurity, $J = 1.5$.

SC exhibits minima. Those positions are determined by the specific strengths of the RSOI and DSOI. When the magnetic impurity is at a peak (valley) of the potential $\frac{\alpha\beta}{2} \sin 2\phi$, the magnitude of the persistent SC increases (decreases) as the $s-d$ exchange interaction strength J increases. This provides us a possible way to control the spin current utilizing the magnetic impurity.

We depict the persistent SC with different RSOI strength α and DSOI strength β in Fig. 11(b) at a fixed J . The symmetry of the persistent SC in the α - β parameter space is still the same as what we reported before in the absence of the magnetic impurity²⁰. The eigenenergy levels become twofold degenerate when α and β are tuned to proper values in the absence of the magnetic impurity, and the contributions

from these two degenerate levels cancel each other and consequently lead to the vanishing SC. This twofold degeneracy will be lifted by the $s-d$ exchange interaction and the levels split into singlet and triplet states. The contributions to the persistent SC from the singlet states ($|0,0\rangle$) are zero while those from the triplet states ($|1,-1\rangle, |1,0\rangle, |1,1\rangle$) states cancel each other so that the total persistent SC is still zero even in the presence of the magnetic impurity. That is why the symmetry is robust against the magnetic impurity. But the magnitude of the persistent SC is suppressed by the magnetic impurity, i.e., the $s-d$ exchange interaction.

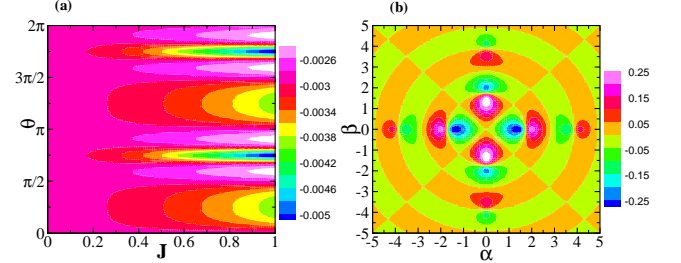


FIG. 11: (Color online) (a) Contour plot of the persistent SC as a function of the strength J of the $s-d$ exchange interaction and the impurity position θ , $\alpha = 3$, $\beta = 2$, and $\phi = 0.5$; (b) Contour plot of the persistent SC as a function of the RSOI strength α and DSOI strength β , $J = 0.5$, $\theta = 0$, and $\phi = 0.5$.

IV. CONCLUSIONS

We have investigated theoretically the spin states and persistent currents (CC and SC) in a 1D ring with an embedded magnetic impurity. The $s-d$ exchange interaction between the electron and the magnetic impurity splits the eigenstates into singlet states and triplet states. The magnetic impurity acts as a δ -barrier (δ -well) for the singlet (triplet) states when $J > 0$, opens energy gaps in the energy spectrum, and suppresses the persistent CC and SC. The competition between the Zeeman terms and the $s-d$ exchange interaction leads to a transition of the electron ground state in the ring. The eigenenergy spectrum, probability distribution, and persistent SC depend sensitively on the position of the magnetic impurity. The symmetry of the persistent SC in parameter space (α - β) is not destroyed by the magnetic impurity.

Acknowledgments

This work was supported by the NSFC Grant No. 60525405 and the knowledge innovation project of CAS.

APPENDIX: THE HAMILTONIAN IN THE COUPLING REPRESENTATION

In the decoupling representation, the basis set is the direct product of the spin states of the electron and the magnetic

impurity $|s_z^e\rangle \otimes |s_z^m\rangle$. The Hamiltonian of a one-dimensional ring with an embedded magnetic impurity can be written as

$$H_{nc} = \begin{array}{c} \begin{array}{c} |\downarrow\downarrow\rangle \\ |\uparrow\downarrow\rangle \\ |\downarrow\uparrow\rangle \\ |\uparrow\uparrow\rangle \end{array} \begin{bmatrix} H_- & 0 & 0 & 0 \\ 0 & H_+ & -\pi J \delta(\varphi - \theta) & 0 \\ 0 & -\pi J \delta(\varphi - \theta) & H_+ & 0 \\ 0 & 0 & 0 & H_- \end{bmatrix}, \end{array} \quad (\text{A.1})$$

where $H_+ = \left(-i\frac{\partial}{\partial\varphi} + \phi\right)^2 + \frac{\pi J}{2}\delta(\varphi - \theta)$ and $H_- = \left(-i\frac{\partial}{\partial\varphi} + \phi\right)^2 - \frac{\pi J}{2}\delta(\varphi - \theta)$. We can transform it to the coupling representation via a unitary operator S which is related to C - G coefficients $S_{m_1 m_2 j m}^{\frac{1}{2} \frac{1}{2}}$.

$$H_c = S^{-1} H_{nc} S,$$

$$S = \begin{array}{c} \begin{array}{c} |0, 0\rangle \\ |1, -1\rangle \\ |1, 0\rangle \\ |1, 1\rangle \end{array} \begin{bmatrix} 0 & 1 & 0 & 0 \\ 1/\sqrt{2} & 0 & 1/\sqrt{2} & 0 \\ -1/\sqrt{2} & 0 & 1/\sqrt{2} & 0 \\ 0 & 0 & 0 & 1 \end{bmatrix}, \quad (\text{A.2})$$

$$S^{-1} = S'.$$

Thus the Hamiltonian in the coupling representation is

$$H_c = \begin{bmatrix} H_S & 0 \\ 0 & H_T I_3 \end{bmatrix}, \quad (\text{A.3})$$

where $H_S = \left(-i\frac{\partial}{\partial\varphi} + \phi\right)^2 + \frac{3\pi J}{2}\delta(\varphi - \theta)$ is the Hamiltonian for the singlet states ($j = 0$), $H_T = \left(-i\frac{\partial}{\partial\varphi} + \phi\right)^2 - \frac{\pi J}{2}\delta(\varphi - \theta)$ is the Hamiltonian for the triplet states ($j = 1$), and I_3 represents the 3×3 identity matrix.

Because of the cylindrical symmetry, the position of the magnetic impurity can be assumed to be $\theta = 0$ without loss of generality.

For the singlet state, the magnetic impurity acts as a δ -potential barrier whose strength is $\frac{3\pi J}{2}$ ($J > 0$). All related eigenstates should be free states in the ring ($E = \kappa^2 > 0, \kappa > 0$), and can be determined by

$$\begin{cases} \left(-i\frac{\partial}{\partial\varphi} + \phi\right)^2 X = \kappa^2 X, 0 < \varphi < 2\pi \\ X(0) = X(2\pi) \\ X'(0) - X'(2\pi) = \frac{3\pi J}{2} X(0). \end{cases} \quad (\text{A.4})$$

The general solution $X(\varphi) = C_1 e^{i(\kappa - \phi)\varphi} + C_2 e^{-i(\kappa + \phi)\varphi}$, we obtain the following transcendental equation:

$$4\kappa[\cos 2\pi\phi - \cos 2\pi\kappa] = 3\pi J \sin 2\pi\kappa. \quad (\text{A.5})$$

The singlet eigenenergies $E = \kappa^2$ can be obtained from the zeros of Eq. (A.5). We further consider the following special cases:

(a) when ϕ is an integer;

The κ values are determined by

$$\sin \pi\kappa = 0 \text{ or } \cot \pi\kappa = \frac{4\kappa}{3\pi J}. \quad (\text{A.6})$$

(b) when ϕ is a half-integer.

The κ values are determined by

$$\cos \pi\kappa = 0 \text{ or } \tan \pi\kappa = -\frac{4\kappa}{3\pi J}. \quad (\text{A.7})$$

For the triplet state electrons, the magnetic impurity acts as a δ -potential well whose strength is $\frac{\pi J}{2}$ ($J > 0$). The lowest triplet state could be a bound state ($E = -\kappa^2 < 0, \kappa > 0$), and the higher states can still be free states extended over the whole ring ($E = \kappa^2 > 0, \kappa > 0$). The free triplet eigenstates can be determined by

$$\begin{cases} \left(-i\frac{\partial}{\partial\varphi} + \phi\right)^2 X = \kappa^2 X, 0 < \varphi < 2\pi \\ X(0) = X(2\pi) \\ X'(0) - X'(2\pi) = -\frac{\pi J}{2} X(0). \end{cases} \quad (\text{A.8})$$

The corresponding transcendental equation can be derived similarly,

$$4\kappa[\cos 2\pi\phi - \cos 2\pi\kappa] = -\pi J \sin 2\pi\kappa. \quad (\text{A.9})$$

The eigenenergy spectrum at the specific magnetic fluxes are:

(a) when ϕ is an integer;

The κ values are determined by

$$\sin \pi\kappa = 0 \text{ or } \cot \pi\kappa = -\frac{4\kappa}{\pi J}. \quad (\text{A.10})$$

(b) when ϕ is a half-integer.

The κ values are determined by

$$\cos \pi\kappa = 0 \text{ or } \tan \pi\kappa = \frac{4\kappa}{\pi J}. \quad (\text{A.11})$$

The triplet bound state can be obtained by substituting κ with $i\kappa$ in Eqs. (A.8), (A.9), (A.10), and (A.11). The corresponding transcendental equation is

$$4\kappa[\cos 2\pi\phi - \cosh 2\pi\kappa] = -\pi J \sinh 2\pi\kappa. \quad (\text{A.12})$$

The eigenenergy spectrum at the specific magnetic fluxes are:

(a) when ϕ is an integer;

The κ values are determined by

$$\coth \pi\kappa = \frac{4\kappa}{\pi J}. \quad (\text{A.13})$$

(b) when ϕ is a half-integer.

The κ values are determined by

$$\tanh \pi\kappa = \frac{4\kappa}{\pi J}. \quad (\text{A.14})$$

The Zeeman terms are diagonal matrix elements in decoupling representation,

$$H_{nc}^Z = \begin{bmatrix} -(g_e + g_m)\phi & 0 & 0 & 0 \\ 0 & (g_e - g_m)\phi & 0 & 0 \\ 0 & 0 & (g_m - g_e)\phi & 0 \\ 0 & 0 & 0 & (g_e + g_m)\phi \end{bmatrix}. \quad (\text{A.15})$$

But in coupling representation it becomes

$$H_c^Z = S^{-1} H_{nc}^Z S$$

$$= \begin{bmatrix} 0 & 0 & (g_e - g_m)\phi & 0 \\ 0 & -(g_e + g_m)\phi & 0 & 0 \\ (g_e - g_m)\phi & 0 & 0 & 0 \\ 0 & 0 & 0 & (g_e + g_m)\phi \end{bmatrix}.$$

(A.16)

Generally speaking, g_e is not equal to g_m , and therefore the singlet $|0,0\rangle$ and triplet $|1,0\rangle$ states are coupled together by the Zeeman terms (see $(g_e - g_m)\phi$ in Eq. (A.16)).

- * Electronic address: [Electronic address:]kchang@red.semi.ac.cn
- ¹ S. A. Wolf, D. D. Awschalom, R. A. Buhrman, J. M. Daughton, S. von Molnár, M. L. Roukes, A. Y. Chtchelkanova, and D. M. Treger, *Science* **294**, 1488 (2001).
 - ² I. Žutić, J. Fabian, and S. D. Sarma, *Rev. Mod. Phys.* **76**, 323 (2004).
 - ³ J. K. Furdyna, *J. Appl. Phys.* **64**, R29 (1988).
 - ⁴ J. Jaroszyński, J. Wróbel, M. Sawicki, E. Kamińska, T. Skośkiewicz, G. Karczewski, T. Wojtowicz, A. Piotrowska, J. Kossut, and T. Dietl, *Phys. Rev. Lett.* **75**, 3170 (1995).
 - ⁵ M. Sawicki, T. Dietl, J. Kossut, J. Igalson, T. Wojtowicz, and W. Plesiewicz, *Phys. Rev. Lett.* **56**, 508 (1986).
 - ⁶ R. Fiederling, M. Keim, G. Reuscher, W. Ossau, G. Schmidt, A. Waag, and L. W. Molenkamp, *Nature* **402**, 787 (1999).
 - ⁷ Y. Ohno, D. K. Young, B. Beschoten, F. Matsukura, H. Ohno, and D. D. Awschalom, *Nature* **402**, 790 (1999).
 - ⁸ E. I. Rashba, *Sov. Phys. Solid State* **2**, 1109 (1960).
 - ⁹ Y. A. Bychkov and E. I. Rashba, *J. Phys. C* **17**, 6039 (1984).
 - ¹⁰ G. Dresselhaus, *Phys. Rev.* **100**, 580 (1955).
 - ¹¹ G. Lommer, F. Malcher, and U. Rössler, *Phys. Rev. Lett.* **60**, 728 (1988).
 - ¹² S. Murakami, N. Nagaosa, and S. C. Zhang, *Science* **301**, 1348 (2003).
 - ¹³ J. Sinova, D. Culcer, Q. Niu, N. A. Sinitsyn, T. Jungwirth, and A. H. MacDonald, *Phys. Rev. Lett.* **92**, 126603 (2004).
 - ¹⁴ M. C. Chang, *Phys. Rev. B* **71**, 085315 (2005).
 - ¹⁵ W. Yang, K. Chang, X. G. Wu, and H. Z. Zheng, *Appl. Phys. Lett.* **89**, 132112 (2006).
 - ¹⁶ L. Besombes, Y. Leger, L. Maingault, D. Ferrand, H. Mariette, and J. Cibert, *Phys. Rev. Lett.* **93**, 207403 (2004).
 - ¹⁷ S. K. Joshi, D. Sahoo, and A. M. Jayannavar, *Phys. Rev. B* **64**, 075320 (2001).
 - ¹⁸ J. B. Xia, *Phys. Rev. B* **45**, 3593 (1992).
 - ¹⁹ J. Splettstoesser, M. Governale, and U. Zülicke, *Phys. Rev. B* **68**, 165341 (2003).
 - ²⁰ J. S. Sheng and K. Chang, *Phys. Rev. B* **74**, 235315 (2006).
 - ²¹ L. Wendler, V. M. Fomin, and A. A. Krokhin, *Phys. Rev. B* **50**, 4642 (1994).